Minireview

Thrombin Inhibitors With Novel Azaphenylalanine Scaffolds and a New P1 Binding Pocket Functionality: Structural Analysis of Binding

Gregor Mlinsek,[1] Rainer Friedrich[2] and Tom Solmajer[1,*]

[1] *National Institute of Chemistry, POB 660, Hajdrihova 19, 1001 Ljubljana, Slovenia*

[2] *Max-Planck-Institute for Biochemistry, Am Klopferspitz 18a, 82152 Martinsried, Germany*

** Corresponding author: E-mail: tom.solmajer@ki.si, Phone: +386-01-4760-277; Fax: +386-01-4760-300*

Received: 15-05-2008

Dedicated to the memory of Professor Ljubo Golič

Abstract

Thrombin, a serine proteinase of the trypsin family, plays a central role in thrombosis and hemostasis. There is a high need for potent, fast, stable and selective direct thrombin inhibitors for oral use, and intensive research in this field is being carried out. Recently, we followed a rational design paradigm for discovery of two novel series of thrombin inhibitors. Firstly, we concentrated on inhibitors with an aza peptide scaffold that mimic the classical tripeptide D-Phe-Pro-Arg structure. A second focus of our work was the search for thrombin inhibitors with uncharged P1 functionalities to optimize the bioavailability and selectivity towards trypsin. Our efforts resulted in several P1 bicyclic arginine mimetics attached to the glycyl-proline amide and pyridinone acetamide scaffold. In this paper we report seven crystal structures of a series of congeneric inhibitors with the novel aza scaffold and with neutral P1 moieties in complex with thrombin. In particular, the requirements for a successful recognition of both inhibitor classes directed at the protein's active-site pocket S1 are discussed based on detailed analysis of their electron distribution and water structure in the pocket.

Keywords: Thrombin, inhibitor, X-ray structure

1. Introduction

Control of platelet aggregation, clot lysis and inhibition of thrombin generation and activity are therapeutic approaches leading to lower cardiovascular morbidity and mortality. The majority of existing reversible thrombin inhibitors are derived from fibrinogen and belong to one of the following chemical groups: tripeptidic reversible transition state mimetics, tripeptidic noncovalent inhibitors, and nonpeptidic inhibitors.[1,2] Two principle-modifying strategies were used in efforts to obtain an orally active drug and resulted in chemically very heterogeneous structures: firstly, the highly basic P1 moiety is kept unchanged, while the P2–P3 part is modified to increase bioavailability; the basic P1 assures an effective binding constant, and this is the approach that also nature favors; all natural inhibitors and substrates possess a highly basic residue – arginine or lysine – at the P1 site. Alternatively, the basicity of the P1 part can be lowered to improve bioavailability, but the loss of potency must be compensated through modifications in the P2–P3 part.[3] E.g. replacing the benzamidine moiety with amino-bicycloaryl brought about increased bioavailability and potency in the low nanomolar range.[4]

In order to introduce novel chemical and biological properties in the classical tripeptide D-Phe-Pro-Arg structure, we incorporated an azapeptide moiety into the central part of the inhibitor.[5] In this way, the conformational flexibility of these molecules was reduced, their stereogenic center eliminated and the *in vivo* stability increased. To improve the bioavailability the basicity at the P1 site was reduced by exchanging benzamidine with benzamidoxime in some of these aza analogues. In order to optimize the occupancy in the S2 pocket, a further se-

ries of compounds was synthesized with binding constants in the nanomolar range.[6]

Investigations in the glycyl-proline amide family of thrombin inhibitors directed toward the S2 pocket have been described in the literature.[7] The P1 moieties reported constitute of a variety of analogs based on the substituted aromatic or aliphatic five or six- membered rings.[8] In order to develop orally bioavailable and selective thrombin inhibitors, we prepared several new heterobicyclic P1 moieties of low basicity. To improve the potency of such inhibitors, various optimization strategies at sites P2 and P3 were attempted: e.g. an additional benzyl sulfonamide group at the P3 moiety was appended to the glycyl-prolyl scaffold, or the glycyl-prolyl moiety at P2 was replaced with the pyridinone acetamide ring,[9–11] which is devoid of cis/trans izomerization and thus conformationally more restricted.

The long and narrow S1 pocket of the thrombin active site ideally accomodates an arginine group as discovered by structural studies of natural inhibitors and substrates. However, functional groups of different degrees of basicity can mimic and bind as a surrogate for arginine e.g.: benzamidine,[12] lysyl,[13,14] cyclohexylamine, benzylamine, aminopiridyl, tiazolyl,[7] indole,[15] guanidinopiperidyl[16] etc. Remarkably, these groups also replace ordered water molecules present in the S1 pocket to different degrees. An analysis of thrombin inhibitors deposited in the RCSB Protein Data Bank[17] to date revealed that the number and position of the water molecules remaining at the bottom of the S1 site close to the residue Asp189 and in the adjacent water channel remain consistenly unchanged upon binding of inhibitors. The main difference in structures of complexes inhibitor-thrombin presented

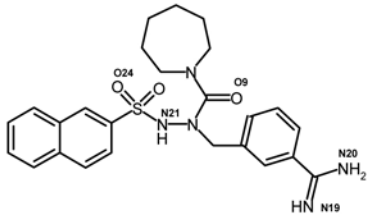

1 (K_i=5nM)

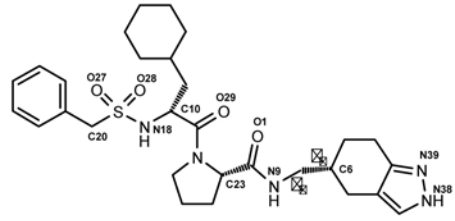

4 (K_i=143nM)

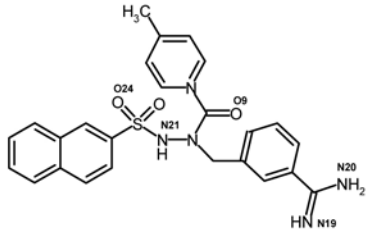

2 (K_i=4nM)

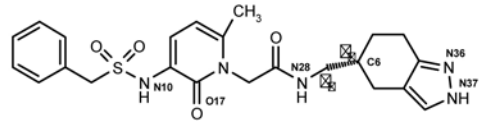

5 (K_i=200nM)

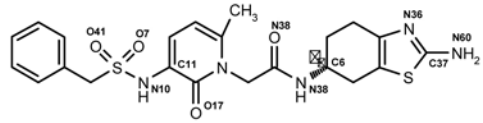

6 (K_i=240nM)

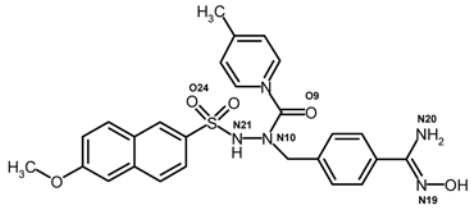

3 (K_i=378nM)

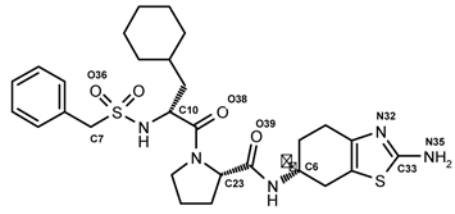

7 (K_i=128nM)

Figure 1. Chemical structures of thrombin inhibitors **1–7**.

here was found in the position of the water molecules close to the Asp189 carboxylate, depending on the structure of the inhibitors' P1 moieties and the way they enter the S1 pocket.

In this paper we summarize the principal findings on the previously reported crystal structures of seven ternary complexes of human -thrombin formed with sulfated hirugen and small molecule thrombin active-site inhibitors that belong to three different families: to the "aza" scaffold family of inhibitors (molecules **1–3**),[6] to the pyridinone acetamide family: molecules **5** and **6,** and to the glycylproline amide family: molecules **4** and **7**.[18–20]

2. Results and Discussion

Thrombin crystals were prepared as described previously.[21]

The crystallization was carried out using the hanging drop vapor diffusion technique and crystals were soaked in a solution containing 1 mM of inhibitor. Coordinates of α-thrombin-hirugen (PDB ID 1HGT)[21] were used as a replacement model. Structure solution and refinement was performed using the standard software [22–27]

The X-ray crystallographic data and the model refinement statistics are summarized in Tables 1 and 2, respectively.

Initial difference electron density maps calculated from the atomic coordinates of the protein after positional and temperature factor refinement revealed the topology of all seven inhibitors and the position of the solvent molecules. The crystal structures were determined to a maximal resolution varying from 1.7 Å to 2.7 Å (Table 1).

In the nonchiral group of molecules, the exact positions of all inhibitors were unequivocally defined by the electron density at 1σ. Absent or weaker electron density

Table 1. X-ray crystallographic data summary*.

Inhibitor	**1**	**2**	**3**	**4**	**5**	**6**	**7**
Resolution range (Å)	20–1.73	20–2.55	20–2.7	20–2.4	20–1.9	20–2.0	20–1.9
Number of observations	362071	69880	56694	75333	192438	113755	91361
Number of theor. possible reflections.	36891	11344	9574	13652	27485	23414	27629
Number of unique reflections	35877	10191	8670	13215	26348	21428	27085
No. of reflections in refinement	34096	9650	8191	12542	25074	20397	25755
Completeness (%) Overall	95.2	94.8	90.4	97.4	95.8	91.4	98.3
Highest resolution shell	97.2	85.3	75.7	99.3	97.7	88.3	98.0
$R_{sym,\ I/\sigma>2:}$ Total	0.045	0.108	0.118	0.132	0.062	0.092	0.058
$R_{sym,\ I/\sigma>2:}$ Highest resolution shell	0.357	0.339	0.358	0.338	0.342	0.319	0.295
Space group	C2	C2	C2	C2	C2	C2	C2
Unit cell parameters							
a (Å)	70.4	69.43	69.89	69.48	69.53	69.47	69.96
b (Å)	71.37	71.36	71.37	71.52	71.71	71.53	71.49
c (Å)	72.58	71.71	71.42	71.97	71.72	71.80	72.18
β (°)	100.37	99.61	99.85	99.84	99.53	99.87	100.15

* – R_{sym} is defined as $\sum_n \sum_i |I_i - \langle I \rangle| / \sum_n \sum_i \langle I \rangle$ where I_i is the *i*th observarion of the *n*th reflection and I is the mean of all observarions of the *n*th reflections.

Table 2. Model refinement statistics*.

Inhibitor	**1**	**2**	**3**	**4**	**5**	**6**	**7**
Number of atoms in the model							
Overall	2618	2506	2481	2602	2590	2688	2663
Protein	2263	2263	2263	2263	2263	2263	2263
Hirudin peptide	86	86	86	86	86	86	86
Inhibitor	34	34	37	39	33	33	39
Water molecules	234	122	90	197	207	294	273
Na^+	1	1	5	5	1	4	2
DMSO	0	0	0	12	0	8	0
RMSD: Bond lengths	0.010	0.0106	0.0105	0.010	0.0108	0.0101	0.0114
RMSD: Bond angles	1.4586	1.5415	1.5407	1.576	1.4174	1.5714	1.7090
Crystallographic R-value	19.82	19.52	19.45	22.60	19.21	19.43	19.98
R_{free}	21.93	24.93	26.45	27.52	22.96	23.70	22.42

* – R_{free} is a statistical value that is calculated as $R = \sum | F_{obs} - F_{calc} | / \sum | F_{obs}|$. It uses a small subset of randomly selected reflections that are set aside from the beginning and not used in the refinement of the structural model.

F_{calc} is a computed expected structure factor amplitude, F_{obs} is an observed value.

was noticed for the benzyl rings in **4** and **7,** respectively. For chiral molecules, the distinction between R and S configurations was resolved using the crystallographic experimental data and quantum-chemical computational approach.[28]

We begin our analysis of the general binding mode of the inhibitors by a description of the inhibitor scaffold positioning in the active site. All inhibitors that are reported here are noncovalent tripeptide mimetics. They bind into the S1 to S4 pockets of the active site of thrombin in two different binding modes: either in a compact more or an extended binding mode. The difference between both types resides primarily in the way their scaffolds are positioned in the respective pockets and thus in the way by which the P1–P3 residues enter and fill the pockets of the active site. In the aza bond family (compact form), the P2 moiety is linked to the scaffold via an amide bond. This leads to a differential binding of the backbones of the inhibitors in the compact vs extended binding mode, which lie as far as 4 Å appart from each other and to a different orientation of the P2 moiety in the S2 pocket (Fig. 2).

The differences in location and orientation of the P1 and P3 parts are less pronounced. This causes in the aza bond series different contacts between the inhibitors and the protein moiety and gives rise to an induced fit of the Trp60D side chain of the S2 pocket. In the glycyl-proline and piridinone acetamide series (extended form), the P2 moiety constitutes a part of the backbone, which links the P1 and the P3 moieties.

2. 1. Thrombin Inhibitors With azaphenylalanine Scaffold

The main novelty of the aza bond inhibitors **1–3** was the elimination of the chiral center and achievement of an increased *in vivo* stability of inhibitors. In inhibitors **1** and **2,** the benzamidine is linked to the backbone of the inhibitor as a 1,3 substituent, which enables its optimal entrance into the S1 pocket and restricts its rotation. The amidine interacts with the Asp189 forming a strong salt bridge, which appears to strongly contribute to the low nanomolar affinity constant. As the

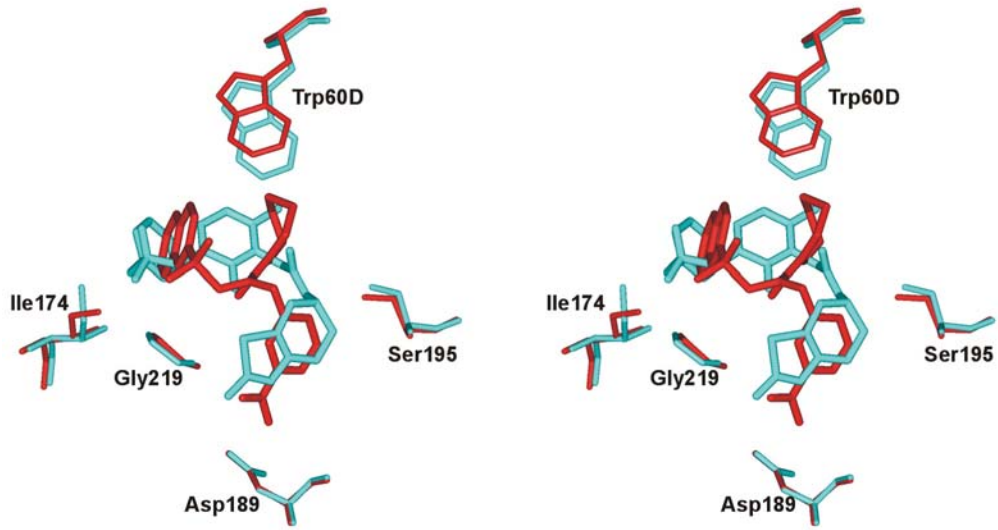

Figure 2. General binding mode of the inhibitors represented by overlapping a compact (red) and an extended binding mode (cyan).

Table 3. Hydrogen bond contacts for inhibitors **1–3**.

Atom (inhibitor)	Residue	Atom	Distance	Atom (inhibitor)	Residue	Atom	Distance	Atom (inhibitor)	Residue	Atom	Distance
1				**2**				**3**			
N20	Asp189	Oδ1	2.82	N20	Asp 189	Oδ1	2.57	N20	Asp 189	Oδ1	2.50
N19	Asp189	Oδ2	2.84	N19	Asp 189	Oδ2	2.50	N20	Ala 190	O	3.07
N19	Ala190	O	3.09	N19	Ala 190	O	3.32*	O9	Gly 216	N	3.09
O9	Gly216	N	3.10	O9	Gly 216	N	3.12	O24	Gly 219	N	3.37*
N21	Gly216	O	2.76	N21	Gly 216	O	2.90	N21	**3**	O9	3.21
O24	Gly219	N	2.94	O24	Gly 219	N	3.17				
N19	Gly219	O	2.81	N19	Gly 219	O	2.70				
N21	**1**	O9	2.65	N21	**2**	O9	2.79				
N20	W5	O	3.02	N20	H2O	12	3.30*				

* a very weak bond

molecules **1** and **2** differ only slightly at the P2 position they display the same set of eight hydrogen bonds (Table 3).

As a consequence of the methyl substituent at the pyrimidine ring of **2,** the inhibitor is pushed down into the S1 pocket, what causes double hydrogen bonds to Asp189 to be shorter for 0.2–0.3 Å with respect to contacts in **1**. Apart from the twined contact with Asp189, both benzamidine nitrogens make contacts with the carbonyl oxygen O of Ala190. One benzamidine nitrogen is also within hydrogen bond distance to Gly219 atom O. Gly219 makes a second contact via its Gly219 N and one of the sulfonamide oxygens, while sulfonamide nitrogen hydrogen bonds Gly216 O. The amide nitrogen of Gly216 forms a bond to the carbonyl oxygen O9 in the S2 pocket. Oxygen atom O9 in turn forms a strong intramolecular hydrogen bond to the sulfonamide nitrogen. This intramolecular bond together with the hydrophobic collapse of the P2 and P3 moieties helps to stabilize the molecule in its compact form.

Molecule **3** posseses a 1,4 substituted benzamidoxime in position P1 and thus a better membrane permeability than **1** or **2** because of its lower basicity. Furthermore, the benzamidoxime moiety is converted to benzamidine *in vivo,* and such molecules can therefore serve as prodrugs. Our *in vivo* tests imply, however, that this conversion is not immediate upon drug absorption.[6] A certain percent of the inhibitor interacts with the thrombin as benzamidoxime and in order to delineate the structural difference in binding to thrombin the present X-ray analysis was nevertheless warranted. In the inhibitor **3,** the 1,4-benzamidoxime group enters the S1 pocket from the same site as the 1,3-substituted benzamidine of **2**. As a consequence, the benzyl ring occupies approximately the same position in both molecules (Fig. 3).

An important consequence of the unfavourable insertion of the 1,4-benzamidine moiety into the S1 pocket is the loss of three hydrogen bonds, in particular the two bonds formed by one of the 1,3 substituted benzamidine nitrogens in **1** and **2** with Asp189 and Ala190. The third hydrogen bond, in **1** and **2** formed between the aza nitrogen N21 and the carbonyl atom O of Gly216, is not observed in **3** as well. The reason for this lies in the planarity of the central part of the inhibitor. At the central aza bond region of **3,** the whole planar triangle tilts for approximately 55 degrees so that N21 moves about 2 Å toward the Trp60D and thus the contact to Gly216 is lost.

These observations lead us to conclude that the loss of the hydrogen bond between the aza nitrogen and the carbonyl O of Gly216 in **3** is the result of a combination of two structural elements, i.e. 1,4 substitution of the benzyl ring and planarity at the central part by the N–N bond. In **3,** the sulfonyl oxygens slightly rearrange without affecting the inhibitor hydrogen bonding scheme, since they remain directed toward the solvent. The loss of these interactions probably contributes to the lower potency of **3** vs. **2** or **1**, respectively. The estimation of the appropriateness of benzamidoxime as a substitution for benzamidine in **1** and **2** thus could not be fully evaluated on structural grounds only. The binding constant of an analog of **3,** where benzamidoxime is 1,3 substituted, is comparable to that of **3**.[6] These findings appear to suggest that the charge of the P1 substituent is more important for the efficacy of binding than the nonoptimal substituent orientation.

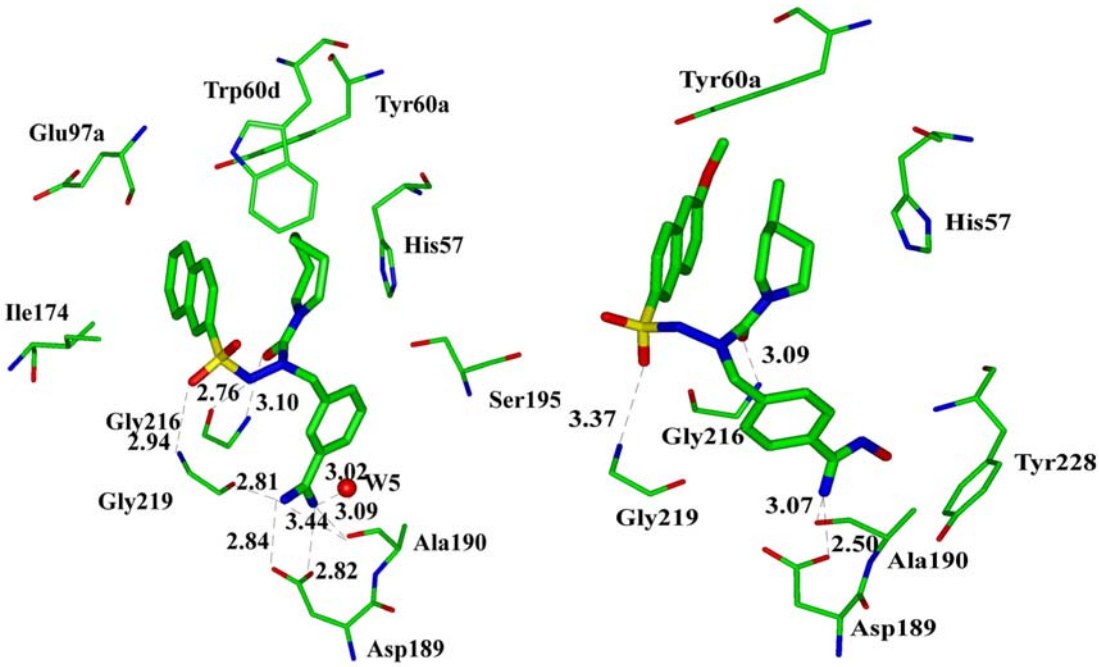

Figure 3. 1,4-benzamidoxime group of inhibitor **3** enters the S1 pocket similar to the 1,3-substituted benzamidine of **2**.

All three molecules bind identically into the S2 pocket and the aryl binding site. The piperidino group of **2** was refined in the chair position. All P2 moieties are oriented parallel with the naphthylsulfonyl of P3. They all bind in parallel orientation to imidazole group of His57 but perpendicular to the phenole and indole moieties of Tyr60A and Trp60D of the S2 pocket. The P2 ring of aza family molecules is perpendicular to the P2 moieties of the other four inhibitors reported here. This orientation is of interest, because Trp60D has to move in order to accomodate for such binding. Atoms Cμ3 and Cξ3 of Trp60D move for 1.85 Å. Although energy is spent for the accommodation of the residue Trp60D, this has no negative influence to the binding constant, which is in the low nanomolar range.

The naphthylsulfonyl rings of molecules **1–3** are coplanar and lie at identical positions.

The methoxy group of **3** placed in the S3 pocket is rotated about 20° out of the plane of the naphthyl ring and oriented toward residues Leu99, Tyr60A and Trp96. No hydrogen bonds are formed to the methoxy oxygen, and only two carbon atoms of Leu99 make close contacts with the group. Since the naphthyl rings of **1–3** occupy identical positions, the methoxy group in **3** does not contribute to the overall binding of the naphthylsulfonyl moiety.

On the basis of crystallographic structure determination we conclude that the reasons for the better binding of **1** and **2** over **3** are at least twofold. First and most important is the presence of the positive charge at P1 in benzamidine. Second, there is a loss of three hydrogen bonds in **3**. The 1,3 benzamidine in **2** allows for good contacts of this inhibitor with Asp189 of thrombin while the para substitution of benzamidoxime in **3** does not. Inhibitor **2** consequently forms two more hydrogen bonds to the protein in the S1 pocket than **3** does. Inhibitor **3** additionally lacks a hydrogen bond with the backbone carbonyl oxygen of Gly216. This is the consequence of the aza functionality in combination with 1,4 benzamidine. Its planarity and thus rigidity hampers effective accommodation of the central part of the inhibitor. No contacts to water molecules in S1 pocket are observed in **3**. However, this is not important since **3** supplants one water molecule with its benzamidoxime oxygen and forms similar contacts to protein as the removed water molecule.

In the case of **3**, only one nitrogen of benzamidoxime forms a hydrogen bond with Asp189 and only two weak bonds with the carbonyl oxygens of Trp215 and Ala190 while a network with seven hydrogen bonds is present in the case of the low nM inhibitor **2** (Table 2).

2. 2. Thrombin Inhibitors With a Pyridinone Acetamide and Glycylproline Amide Scaffold

The important novelty of molecules **4–7** is the introduction of a heterobicycle at P1 with intention to increase selectivity and bioavailability because of its lower basicity. The structural fragments P2 and P3 have been used earlier.[7,9–11] The crystal structures of all four high nanomolar inhibitors show the backbones at P2 to P3 to bind in an extended antiparalel shape to the active site cavity. Despite the high similarity of the overall binding mode, there are important differences in the binding of parts of individual inhibitors, which are described below.

2. 2. 1. Hydrogen Bonds in Heterobicyclic P1 Inhibitors

As mentioned before molecules **4–7** were prepared as racemic mixtures regarding the stereogenic center at the C6 of the 4,5,6,7 tetrahydrobenzyl ring. Electron density clearly selects the R configuration of both piridinone molecules **5** and **6** while it supports R or S configuration of molecules **4** and **7**. As the hydrogen bond pattern changes with the configuration we present hydrogen bonds for both configurations of **4** and **7** (Table 4).

Molecules **4–7** form hydrogen bonds to the backbone of the protein, to the catalytic triade and have a hydrogen bond network at the S1 pocket. All four molecules bind in an antiparallel mode to the backbone of thrombin

Table 4a. Hydrogen bond contacts for inhibitors 4 and 5. * a very weak bond, # lost contact, $^{++}$ not a hydrogen bond due to inappropriate angle.

Atom (inhibitor)	Residue	Atom	Distance – R config.	Distance – R config.	Atom (inhibitor)	Residue	Atom	Distance
	4				**5**			
N38	Asp 189	Oδ1	2.59	2.72	N37	Asp 189	Oδ1	2.45
N38	Asp 189	Oδ2	2.57	2.95^{++}	N36	Asp 189	Oδ2	2.90
N39	Asp 189	Oδ1	2.69^{++}	2.67	N37	Ala 190	O	3.36
N39	Ala 190	O	3.24	3.09	N36	Ala 190	O	3.33
O29	Gly 216	N	3.26	3.20	N36	Gly 219	O	3.10
N18	Gly 216	O	3.10	3.48*	N28	Ser 195	Oγ	2.89
O27	Gly 219	N	3.08	3.28	N28	Ser 214	O	3.23
N9	Ser 195	Oγ	4.13#	3.51	O17	Gly 216	N	3.05
O28	W63	O	3.02	3.34*	N10	Gly 216	O	3.00
N38	W34	O	3.55*	3.40*	N37	W184	O	3.27
					N36	W184	O	2.85

Table 4b. Hydrogen bond contacts for inhibitors **7** and **6** (symbols *,#,++ same as in Table 4a).

Atom (inhibitor)	Residue	Atom	Distance – R config.	Distance – R config.	Atom (inhibitor)	Residue	Atom	Distance
7					**6**			
O39	His 57	Nδ2	4.18#	3.06	N60	Asp189	Oδ2	2.89
N35	Asp 189	Oδ1	2.85	2.71	N60	Gly219	O	2.80
N35	Ala 190	O	3.41*	3.35*	N36	Ala190	O	3.23
O39	Ser 195	Oγ	4.13#	2.80	N28	Ser195	Oγ	3.09
O36	Gly 219	N	3.01	3.29	N28	Ser214	O	2.91
N32	Gly 219	O	3.11	3.01	O17	Gly216	N	3.27
N32	Ala 190	O	3.32	3.55*	N10	Gly216	O	3.13
O38	Gly 216	N	3.26	3.61*	O27	W73	O	2.61
O39	W95	O	4.00#	3.25	O41	W300	O	3.46*
O39	W210	O	3.62*	3.16	N36	W15	O	2.66
N35	W5	O	3.41*	3.33*	O7	W215	O	3.47*
					O7	W107	O	3.42*
					O7	W140	O	3.19

with bonds to Gly216 and Gly219. Contacts to Gly216 atom N are formed by carbonyl oxygens of pyridinone or proline. This bond in **7** is very weak, however (3.61 Å). Gly216 forms in **5** and **6** an additional bond to sulfonamide oxygen. The reason for the absence of this bond in **4** and **7** is that the benzylsulfonamide moiety oxygens form contacts to N Gly219 instead. Gly219 atom O forms a hydrogen bond to the P1 nitrogen of **5, 6** and **7**. In **4** this bond is observed only in the structure of the R enantiomere. In **5** and **6** we note an additional bond between the amide nitrogen N28 and the backbone residue Ser214 atom O. N28 forms also a hydrogen bond to the Ser195 atom Oγ. In **7** the carbonyl oxygen O39 of the peptide bond between P1 and P2 moieties forms a hydrogen bond to Ser195 atom Oγ in the S configuration only, while it can not be demonstrated in the R enantiomere. In **4** the S configuration shows a hydrogen bond between the amide nitrogen and Ser195 atom Oγ while the R configuration shows only a very weak contact between the carbonyl oxygen and Ser195 atom Oγ(3.57 Å). The carbonyl oxygen O39 of the S enantiomere of **7** displays another hydrogen bond to Nξ of the residue His57 of the catalytic triad. This is the consequence of 90 degrees rotation of the peptide bond between the P1 and P2 moiety toward the catalytic triad. This rotation is documented also in the R configuration of the molecule **4**. However, in **4** no contact to His57 is formed.

All four inhibitors also show contacts to Asp189 and Ala190. In **4** and **5** where charge is distributed between both nitrogens of the P1 part twined contacts are formed to Asp189 (Oδ1 and Oδ2). In **6** and **7** only one contact with Asp189 can be documented. The reason for this is in the way how the P1 moieties of **6** and **7** enter the S1 pocket. Both rings lie in the same plane but their longitudinal axes form an angle of approximately 33 degrees. The amino nitrogens are thus more than 2Å appart and form contact to different carboxyl oxygen atoms of Asp189. In **5** both nitrogens are in contact with Ala190 atom O while in **4** only one contact is seen because of a slightly different rotation of P1 in **4** and **5.** Similarly, one contact is present also in inhibitors **6** and **7**.

In all seven structures a conserved water of the oxyanion hole was detected, which binds to Gly193 atom N and Ser195 atom Oγ. Aza bond inhibitors and pyridinone acetamide inhibitors are devoid of the contact to this water molecule. Interestingly, this contact is observed with **7** refined in S configuration and **4** refined to R configuration. In this case hydrogen bonds are due to the specific position of carbonyl oxygen O1 of **4** and O39 of **7**. In this way **4** and **7** are indirectly bound to Gly193 and Ser195. The analogous carbonyl atoms of **5** and **6** are rotated for 90 degrees toward the surface of the protein while aza bond inhibitors are due to the different backbone even more distant from the oxyanion hole residues. Oxygen O27 of **6** forms a hydrogen bond with a water W73. This water molecule makes a direct hydrogen bond to Oε1 Glu192 and indirect bonds to the Ser195 and Gly193 through the water of oxyanion hole. In **5** such a water molecule was not detected.

In summary, the crystallographic refinement implies that molecules **5** and **6** bind in R configuration while for **4** and **7** both R and S configurations are probably possible. Electron density of **7** is slightly more consistant with S configuration while QM/MM calculations argue for the R configuration as the more probable configuration for **4**.[28] The heterobicyclic ring of **4** and **5** binds the S1 pocket deeper than the ring of **6** or **7**. The location of the sulphur atom in **6** and **7** is different.

Inhibitors with glycoproline scaffold fill the S2 pocket slightly differently as the inhibitors of piridinone acetamide core. The proline binds aproximately 1.5 Å closer to His57. Orientation of the peptide bond between the P1 and P2 parts of molecules **7** and **4** differs to that of **5** and **6**.

The aryl binding site binds the benzyl ring in the case of **5** and **6** but cyclohexyl of **4** and **7** molecule.

Differences in the hydrogen bonding network are mainly in number and strength of the bonds to the surrounding water molecules and to residues in the S1 pocket. Inhibitor **7** has also an additional bond to the His57 atom Nε2 of the catalytic triad.

Tautomeric effects in **4** and **5** probably influence the binding of these inhibitors. The distribution of the positive charge between both indazole nitrogens calls for an orientation where both nitrogens are in energetically equivalent position with respect to Asp189. As these nitrogens do not have a very basic character, the unprotonated states are relatively important. However, the energetically more favourable deprotonated state has probably a different conformation, i.e. rotated for 180 degrees with respect to the former. The free rotation about the bonds α0 and α1 above the heterobicyclic ring probably permits for these changes. This case in principle resembles a situation where an unfavourable binding of one enantiomere can be the reason for a low Ki of a racemic mixture although the other enantiomere has a much better bonding constant. This can be a part of the answer to the relatively weak binding constant of these two inhibitors.

2. 2. 2. Interactions in the S1 Pocket

The four inhibitors belonging to the glyco-proline amide and piridinone acetamide type possess a stereogenic center at the atom C6 of the 4,5,6,7 tetrahydrobenzothiazole and the 4,5,6,7 tetrahydroindazole ring, respectively, which are located at the entrance of the S1 pocket (Fig 2). The racemic samples used during the experiment were an unknown mixture of both enantiomeres. Furthermore, both P1 functional groups also have the ability to undergo conformational shifts from "up" to "down" in the upper part of the tetrahydrobenzene ring. Therefore, we had to assume that these inhibitors bind with either configuration into the active site. The determination of the preferential binding configuration was not straightforward in all four cases. Molecules **4** and **7** additionally possess two chiral centers at C10 and at C23. It has been determined that they have R and S configurations [18,19] respectively, and this data has been used in the structure determination.

2. 2. 3. Molecules 6 and 7

Molecule **6** binds preferentially with its R configuration. The difference electron density map calculated for the S configuration shows more positive and negative electron density than in the case of the R-enantiomer and is thus less likely to represent the correct solution. The amide bond between P1 and P2, oriented as in the inhibitors containing proline (PPACK,[29] L371912[30]), points away from the surface of thrombin and projects between the residues Trp215 and Glu192. It forms a hydrogen bond to W73, which in turn contacts Glu192 atom Oε1. The sulphur atom is in the energetically unfavourable location making a close contact to Gly219 atom O(3.1 Å). The location of the sulphur atom at the bottom of the S1 pocket is clearly defined by its stronger density. The unfavourable contact is partly alleviated by the weak hydrogen bond to water molecule W252 (3.4 Å) as a hydrogen acceptor. W252, however, forms no further contacts neither with the protein or with other water molecules. Interestingly, such an energetically unfavourable location has been described previously[29] for the sulphur in the S1 pocket of the urokinase plasminogen activator.

The orientation of the P1 moiety is thus influenced by the size of the heterobicycle, location of the charge at the side of the ring, ring coupling directly to an amide bond where rotations are possible around dihedral α0 only. The 3-nitrogen atom is equally distant to both Asp189 carboxyl oxygens. However, as this protonation centre is located 4.4 Å away from the Asp189, the interaction of tetrahydrobenzothiazole does not have the character of a salt bridge. There is only a weak hydrogen bond between the 2-amino nitrogen atom and the Asp189 atom Oδ2 of protein.

The chemical structure of inhibitor **7** differs from **6** in the P2 and P3 positions, while P1 is the same. Nonetheless, in the solved structure there are also differences within the P1 region, i.e. in the position of the P1 ring in the S1 pocket and in the position of the P1–P2 amide bond. The heterobicyclic P1 ring is coplanar with the ring of **6,** but is flipped for 180 degrees. The sulphur atom of **7,** situated on the opposite sites of the S1 pocket, forms different contacts to the surrounding Val213, while the sulphur of inhibitor **6** points toward the Gly216. The heterobicycles of **6** and **7** lie somewhat crossed, with the axes form approximately 30 degrees. The terminal NH_2 groups are thus 2.3 Å apart, what is of importance for hydrogen bonding with Asp189. Inhibitor **7** forms contacts with both Oγ atoms of the aspartic residue, while **6** only with O2. As these rings can probably rotate to a certain extent this structure probably shows also the other possi-

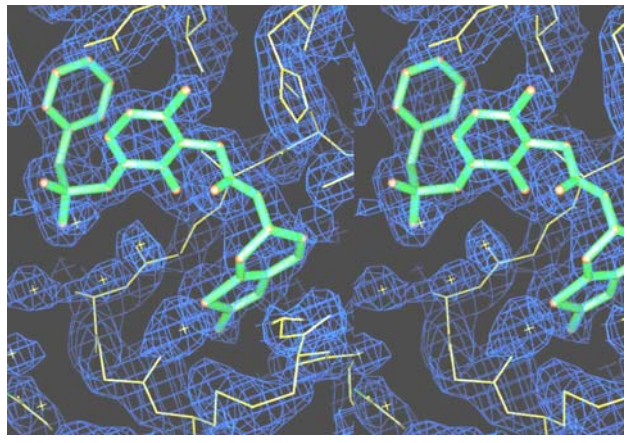

Figure 4. inhibitor **7** with (2|Fo| – |Fc|) and (|Fo| – |Fc|) maps of electron density contoured at 1. 0 σ.

ble but less favourable conformation of **6**. In this orientation, the sulphur atom forms a weak hydrogen bond to W5 (3.49 Å), while the protonated 3-nitrogen is in hydrogen bond distance to Gly219 ATOM O(3.01 Å). The electron density accounting for the sulphur atom is shown in Fig. 4. The sulphur of the same but isolated bicyclic P1 ring (PDB ID 1C5N)[29] attains exactly the same position as in **7**.

As the sample was a racemate, the experimental electron density might account for both of them. The reason lies in the 4,5,6,7-tetrahydrobenzothiazole ring of these inhibitors which has the ability to undergo up to down shifts at C6. Thus, both configurations can adopt the required conformation of the active site. Nevertheless, the electron density is more consistent with the S configuration although R configuration could not be entirely excluded. At the P1 site, both models fit equally well into the electron density but the refinement of the R enantiomere gave an orientation which is outside the electron density at the aryl binding site. The S configured compound shows a perpendicular turn of the amide bond between the P1 and P2 moieties (Fig. 4). The carbonyl oxygen thus points toward the catalytic triad and makes contacts to His57 atom Nξ2(3.05 Å) and Ser195 atom Oγ (2.8 Å).

This may add to the efficacy of this inhibitor, which has the lowest value of binding constant in these four high nanomolar inhibitors. In the R configuration, the amide bond turn is also observed but the contact to His57 or Ser195 is absent. The ability of up/down shifts, R and S configurations, the site of entrance of P1 ring, its orientation (orientation of the sulphur and the charged nitrogen at the side of the ring) and the orientation of the amide bond between P1 and P2 and thus carbonyl oxygen are apparently interdependent.

2. 2. 4. Molecules 4 and 5

P2 and P3 moieties of **5** are structurally identical as in **6** and they also bind identically in both cases. There are two differences to **6**. Firstly, tetrahydrobenzothiazole ring is substituted by the tetrahydroindazole and secondly, 2-amino nitrogen is absent but an additional methyl is added in the peptidomimetic backbone so that the overall length of the P1 part remains unaltered. Nitrogens of indazole ring form a tautomeric system so that charge is distributed between both rings. As this is at the bottom of the ring, positively charged substituent P1 can achieve a direct contact with Asp189. Final 2Fo–Fc electron density map is compatible with the R configuration of the P1 ring as in **6**.

In spite of the fact that P1 moiety of the inhibitors **4** and **5** are equal, the determination of the most probable structural form bound into the active site was more difficult in the case of the inhibitor **4** for several reasons. First, there is a change of orientation of the amide bond between P1 and P2 with respect to configuration as in **7**. Second, the electron density was of approximately the same quality for both, R and S enantiomers. Furthermore, it was difficult to establish the most probable conformer of the P1 moiety since the P1 moiety of the **4** can rotate around the α0 and α1 dihedral and has thus more conformational freedom. According to the calculated pKa of 4.0 (www.acd.labs) the 1-nitrogen of tetrahydroindazole is in the uncharged form. In view of the tautomeric equilibria between indazole nitrogens two conformations of each configuration have to be considered.

2. 2. 5. Interactions of the scaffold and the P2 moiety

The proline and piridinone rings lie coplanarlly below the YPPW loop of thrombin S2 pocket. The piridinone rings in molecules **5** and **6** are positioned at exactly the same place. Proline ring binds approximately 1.5 Å closer to His57, the Cδ of proline occupying the place of the methyl group of the **5** or **6**. Both rings are coplanar with Trp60D and perpendicular to Tyr60A and His57. They are also perpendicular to the piperidino P2 part of the aza family of molecules, which stand parallel to His57. This is an important difference observed between the two binding modes – extended and a more compact one.

2. 2. 6. Interactions in the Aryl Binding Site

It was reported already that the cyclohexyl part and not the benzyl part of the inhibitor **4** or **7** – like molecules binds to the aryl binding site.[30] Our structural studies confirm this finding. Cyclohexyl arm of **4** and **7** has less conformational freedom and a higher lipophilicity than the benzyl ring and binds preferentially into the aryl binding site. In molecules **5** and **6** the aryl binding site is occupied by the benzyl ring, however. Benzylsulfonamide arm is longer than the cyclohexyl. The C11 atom of the **6** occupies approximately the same site as the C10 atom of the **4**. This leads to a slightly different way of entrance of the cyclohexyl ring in the aryl binding site as compared to that of the benzyl ring in the case of **5** or **6**. The angle of the benzyl ring planes of **5** or **6** and cyclohexyl ring of **4** or **7** attains approximately 50 degrees. Electron density of the benzyl ring is well defined at 1 σ for the molecules **5** and **6**. In **4**, however, there is no electron densitiy for the benzyl ring and in **7** the electron density for the benzyl ring is adequately seen at 0.8 σ only and is missing at the C7 atom between the benzyl ring and the sulphonyl group. This weaker density or its absence implies that there is a rotation of the benzyl ring around the bonds between the sulphonyl group and the ring. Such rotation probably precludes a succesfull binding. Surprisingly, this substituent apparently can not occupy an alternative binding place. It was expected that the benzylsulfonamide group of **4** and **7** would bind into the region bordered by Trp60D above, Cys191–Cys220

disulfide linkage below, the side chain carbons of Glu192 and the P1 moiety of the inhibitor itself at the back. Such binding mode was reported previously.[7] In that case benzyl ring of the benzylsulfonamide functionality binds perpendicular to the 6-amino cyclohexane ring (P1) of the inhibitor. Distances between them are within 3.4–3.9 Å. P1 moiety at the back of the pocket is thus probably involved in the hydrophobic collapse with a neighbour part (P3) of the inhibitor – a phenomenon similar to the one observed in the Argatroban/NAPAP family of compounds[31–33] where P2 and P3 moieties ‚collapse'. Sulphonamide oxygens of **4** and **7** form a hydrogen bond to N Gly219. This indicates that the initial part of the benzylsulfonamide arm directs toward the region described above. In the inhibitor **7** the ring is seen at 0.8 σ but the density of the bridging carbon atom to the sulphonamide group is absent. Benzyl ring in **7** occupies the position close to the carbon atoms of the side chain of Glu172 (the closest contact is 3.77 Å). Binding at this position appears neither to improve nor to alleviate the efficacy of binding. This conclusion is derived from the comparison of the molecules **5** and **6,** which possess pyridinone acetamide at P2 and the same P1 parts but no benzylsulfonamide arm. Their affinity is of the same order of magnitude.

The 4, 5, 6, 7 tetrahydrobenzene ring of the inhibitor **7** is rotated for 45 degrees with respect to the 6-amino cyclohexane plane and Trp60D ring. The positive charge of the weakly basic thiazolamino functionality is located at the side 3-nitrogen and not at the terminal aniline type nitrogen. The rotation of this P1 ring is thus more restricted than rotation of 6-amino cyclohexane ring. The orientation of the P1 ring of **7** probably precludes effective interaction with the benzylsulfonamide group and consequently partial disorientation of the latter (seen at 0.8 σ). Favourable hydrophobic contacts are prevented also in **4** where the P1 ring is rotated for 90 degrees with respect to Trp60D. The electron density of the benzyl ring of **4** is absent.

The reason for the absence of the favourable contact is thus in the interaction pattern of tetrahydroindazole of **4** and tetrahydrobenzotiazole of **7** at the bottom of S1 pocket. It is most probably the combination of the size of P1 rings, location of the charge at the side of the rings (**7**) and distribution of charge within the ring (**4**).

2. 3. Structural Motives of the Water Molecules at the Bottom of the S1 Pocket

When P1 parts occupy the S1 pocket they replace water molecules present in the apo structures of thrombin. As they are of different structures and as they enter the pocket from different sites and under different angles, they occupy different positions at Asp189 and supplant a different number of water molecules. The number and position of the water molecules, remaining at the bottom of the S1 site left and right to the Asp189 and in the water channel after the binding of the inhibitor, stay remarkably unchanged. Nevertheless, three distinct patterns can be observed with respect to the presence or absence of water molecule between the P1 moiety and Tyr228. Our inhibitors possess four different P1 moieties and cover all three motifs.

The water pattern most frequently observed is the one present in **1**, **2, 5** and **7**. A highly conserved water molecule acquires the position in the direction toward Tyr228 (Fig. 5a). In **2** it forms hydrogen bonds to Phe227 atom O(3.01 Å) and inhibitor's N20 (3.30 Å) and also weak electrostatic interactions to Trp215 atom O(3.66 Å) and aromatic Tyr228. In other three inhibitors this water molecule occupies an identical position and forms weaker or stronger contacts to the same residues in the surroundings. This water molecule is present in the majority of the thrombin-inhibitor structures in the RCSB protein data bank[17.]

In the second motif this water molecule is absent (Figure 5b). In **3,** for example, it is replaced by the hydroxyl group of the benzamidoxime. This hydroxyl oxygen occupies the exact position of this water and thus also retains the contacts with O Phe227, O Trp215 and Tyr228. Some of structures where this water is absent as well are PDB ID 1ETT, PDB ID 1C4Y, PDB ID 1C5N and PDB ID 1HDT. In all of these structures the P1 moiety protrudes as in **3** toward Tyr228 and supplants the water molecule.

In the third pattern represented by inhibitor **6** an additional water molecule is present (Fig. 5c). It is positioned between the highly conserved water and the inhibitor. The former forms additionally a hydrogen bond to N Phe227 and to the additional water molecule. The latter forms hydrogen bonds to Asp189 atom O, Ala190 atom O, Ala190 atom O, inhibitor's N36 and N60. A similar binding motif is observed also in structures PDB ID 1AE8, PDB ID 1AFE, PDB ID A46 and PDB ID 1D9I. In the first three complexes P1 is a lysyl residue which occupies less volume than other more branched P1 parts leaving room for another water molecule.

In general it is assumed that because of the high entropic cost of trapping highly mobile water molecules, an interface that leaves no space between the interacting protein and the ligand will necessarily give a higher binding affinity than one in which the interface contains gaps filled by water.[34] In certain molecular systems ligands that displace water molecules indeed are highly potent inhibitors.[35,36] In our system, however, water molecules do not seem to play an important role. Molecule **3** which supplants the highly conserved water molecule toward Tyr228 binds with high nM affinity as does its 1,3 analogue. The entropic gain for replacing the conserved water molecules and introducing a direct contact between the inhibitor and thrombin apparently has no net contribution to

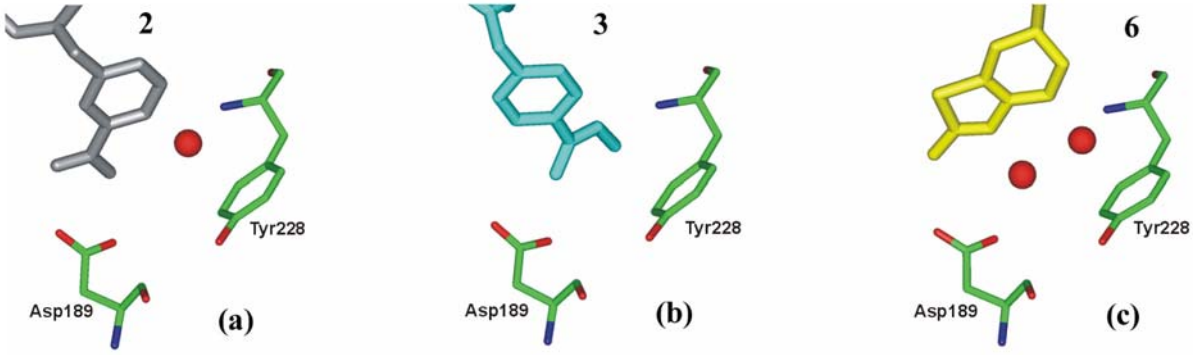

Figure 5. Three motifs of water molecules at the bottom of the S1 pocket observed in inhibitors 1–7.

free energy of binding in this case. On the other hand **6,** which leaves one additional water in front the Asp189, has an affinity that is neither better nor worse than the affinity of related molecules. This is in agreement with the view that thrombin uses water molecules to steer the carboxylate of Asp189[37] and to extend the range of ligands that can bind to the protein.[38] This observation is also in concurrence with the results of our theoretical calculation that the crucial contribution to the efficacy of binding in the S1 pocket arises form the ionic contact between the inhibitor and Asp189.[28] Nevertheless, this observation proves that there is space at the bottom of the S1 pocket for different orientations and sizes of P1 moieties regardless of whether they are charged or uncharged.

3. Conclusions

Molecules **1–3** with azaphenylalanine tripeptide scaffold exhibit a similar binding mode as other inhibitors from the Argatroban/NAPAP family.[1,2,38,39] However, the central planarity of these molecules causes specific adaptation of the central part of the molecules to the surface of thrombin. Molecules **1** and **2** can attain a suitable conformation and preserve low nanomolar binding affinity with an improved *in vivo* behaviour.

The optimization strategy in the glycyl proline family was, to introduce a benzylsulfonamide functionality. Surprisingly, this does not bring much enhancement in potency. The reason for this lies probably in the absence of an effective intramolecular hydrophobic interaction with the P1 moiety as documented before. The reason for this absence is probably the rigid mode of binding of the P1 moiety, due to charge location and size of P1 rings. These observations are indirectly a proof for the influence that the P1 moiety can have on the binding of other parts of the inhibitor and stresses the importance of intramolecular contacts in this family of molecules.

Due to the lower basicity, molecules **4**, **5**, **6** and **7** form weaker electrostatic contacts to Asp189. Although the solvation cost of the uncharged P1 moieties decreases, Coulomb interaction increases relatively more so that the overall electrostatic contribution for the P1 moiety-protein and inhibitor-protein turns positive and thus unfavourable. Our quantitative results show that in molecules with uncharged P1 residue the complexation with thrombin is determined by forces other than electrostatics, which is in agreement with the need to optimize such inhibitors at hydrophobic P2 and P3 moiety.

4. Acknowledgements

G.M. would like to express his sincere gratitude to Professor W. Bode (Martinsried), who generously accepted him in the lab and shared the knowledge in the field. We would like to thank Dr. D.Banner (Roche), who kindly provided the coordinates of the complex napsagatran-human α-thrombin, and our colleagues, Dr. J. Richardson (MPI, Martinsried), and Drs. J. Mavri and D.Kocjan (NIC, Ljubljana) for helpful comments and discussions.

5. References

1. J. M. Fevig, R. R. Wexler, *Annu. Rep. Med. Chem* **1999**, 81–100.
2. J. P. Vacca, *Annu. Rep. Med. Chem.* **1998**, 81–90.
3. J. B. Rewinkel, H. Lucas, M. J. Smit, A. B. Noach, T. G. van Dinther, A. M. Rood, A. J. Jenneboer, C. A. van Boeckel. *Bioorg. Med. Chem. Lett.* **1999**. *9*, 2837–2842.
4. J. B. Rewinkel, A. E. Adang, *Curr. Pharm. Des.* **1999**, *5*, 1043–1075.
5. A. Zega, G. Mlinsek, P. Sepic, S. Golic Grdadolnik, T. Solmajer, T. Tschopp, T. B. Steiner, U. Urleb, *Bioorg. Med. Chem.* **2001**. *9*, 2745–2756
6. A. Zega, G. Mlinšek, T. Solmajer, A. Trampuš-Bakija, M. Stegnar, U. Urleb, 7. *Biorg. Med. Chem. Lett*., **2004,** *14,* 1563–1567.
7. T. J. Tucker, W. C. Lumma, A. M. Mulichak, Z. Chen, A. M. Naylor-Olsen, S. D. Lewis, R. Lucas, R. M. Freidinger, L. C. Kuo,. *J. Med. Chem.* **1997**, *40,* 830–832.

8. D. M. Feng, S. J. Gardell, S. D. Lewis, M. G. Bock, Z. Chen, R. M. Freidinger, A. M. Naylor-Olsen, H. G. Ramjit, R. Woltmann, E. P. Baskin, J. J. Lynch, R. Lucas, J. A. Shafer, K. B. Dancheck, I. W. Chen, S. S. Mao, J. A. Krueger, T. R. Hare, A. M. Mulichak, A. M. J. P. Vacca, *J. Med. Chem.* **1997**, *40,* 3726–3733.
9. P. E. Sanderson, K. J. Cutrona, B. D. Dorsey, D. L. Dyer, C. M. McDonough, A. M. Naylor-Olsen, I. W. Chen, Z. Chen, J. J. Cook, S. J. Gardell, J. A. Krueger, S. D. Lewis, J. H. Lin, B. J. Lucas, Jr., E. A. Lyle, J. J. Lynch, Jr., M. T. Stranieri, K. Vastag, J. A. Shafer, J. A. J. P. Vacca,. *Bioorg. Med. Chem. Lett.* **1998**, *8,* 817–822.
10. P. E. Sanderson, T. A. Lyle, K. J. Cutrona, D. L. Dyer, B. D. Dorsey, C. M. McDonough, A. M. Naylor-Olsen, I. W. Chen, Z. Chen, J. J. Cook, C. M. Cooper, S. J. Gardell, T. R. Hare, J. A. Krueger, S. D. Lewis, J. H. Lin, B. J. Lucas, Jr., E. A. Lyle, J. J. Lynch, Jr., M. T. Stranieri, K. Vastag, Y. Yan, J. A. Shafer, J. P. Vacca. *J. Med. Chem.* **1998**, *41,* 4466–4474.
11. P. E. Sanderson, D. L. Dyer, A. M. Naylor-Olsen, J. P. Vacca, S. J. Gardell, S. D. Lewis, B. J. Lucas, E. A. Lyle, J. J. Lynch, A. M. Mulichak, *Bioorg. Med. Chem. Lett.* **1997**, *7,* 1497–1500.
12. J. Sturzebecher, P. Walsmann, B. Voigt, G. Wagner. *Thromb. Res.* **1984**, *36,* 457–465.
13. G. De Simone, G. Balliano, P. Milla, C. Gallina, C. Giordano, C. Tarricone, M. Rizzi, M. Bolognesi, M., P. Ascenzi. *J. Mol. Biol.* **1997**, *269,* 558–569.
14. R. St Charles, J. H. Matthews, E. Zhang, E., A. Tulinsky *J. Med. Chem.* **1999**. *42,* 1376–1383.
15. J. A. Malikayil, J. P. Burkhart, H. A. Schreuder, R. J. Broersma, Jr., C. Tardif, L. W. Kutcher, III, S. Mehdi, G. L. Schatzman, B. Neises, B., N. P. Peet,. *Biochemistry* **1997**, *36,* 1034–1040.
16. R. Krishnan, E. Zhang, K. Hakansson, R. K. Arni, A. Tulinsky, M. S. Lim-Wilby, O. E. Levy, J. E. Semple, T. K. Brunck, *Biochemistry* **1998**, *37,* 12094–12103
17. H. M. Berman, J. Westbrook, Z. Feng, G. Gilliland, T. N. Bhat, H. Weissig, I. N. Shindyalov, P. E. Bourne The Protein Data Bank Nucl. Acids Res. **2000,** *28,* pp. 235–242 (2000) and URL www. pdb. org.
18. P. Marinko, A. Krbavcic, G. Mlinsek, T. Solmajer, A. Trampuš Bakija, M. Stegnar, J. Stojan, D. Kikelj *Eur. J. Med. Chem*. **2004**, *39,* 257–265.
19. L. Peterlin-Masic, G. Mlinsek, T. Solmajer, W. Bode, A. Trampus Bakija, M. Stegnar, D. Kikelj, *Bioorg. Med. Chem. Lett.* **2003,** *13,* 789–794.
20. L. Peterlin-Mašič, A. Kranjc, P. Marinko, G. Mlinšek, T. Solmajer, M. Stegnar, D. Kikelj, *Bioorg. Med. Chem. Lett.* . **2003**, *13,* 3171–3179.
21. E. Skrzypczak-Jankun, V. E. Carperos, K. G. Ravichandran, A. Tulinsky, M. Westbrook, J. M. Maraganore, *J. Mol. Biol.* **1991**, *221,* 1379–1393.
22. A. G. W. Leslie, *Newsletter on Protein Crystallography,* **1992***, 26, Science and Engineering Research Council, Daresbury Laboratory, Warrington, U. K.*
23. W. Kabsch, *J. Appl. Cryst.* **1988***, 21,* 916–924.
24. J. Navaza, *Acta Cryst.* **1994**, *A50,* 157–163.
25. SYBYL 6. 7, Tripos Inc., 1699 South Hanley Rd., St. Louis, Missouri, 63144, USA.
26. D. Turk, Ph. D. Thesis, **1992**. Technische Universitaet Muenchen
27. A. T. Brunger, P. D. Adams, G. M. Clore, W. L. DeLano, P. Gros, R. W. Grosse-Kunstleve, J. S. Jiang, J. Kuszewski, M. Nilges, N. S. Pannu, R. J. Read, L. M. Rice, T. Simonson, G. L. Warren, *Acta Cryst.* **1998**, *D54,* 905–921.
28. G. Mlinsek, M. Oblak, M. Hodoscek T. Solmajer J. Mol. Model. **2007,** 13:247–254.
29. B. A. Katz, R. Mackman, C. Luong, K. Radika, A. Martelli, P. A. Sprengeler, J. Wang, H. Chan, L. Wong *Chem. Biol.* **2000**, *7,* 299–312.
30. T. A. Lyle, Z. G. Chen, S. D. Appleby, R. M. Freidinger, S. J. Gardell, S. D. Lewis, Y. Li, E. A. Lyle, J. J. Lynch, A. M. Mulichak, A. S. Ng, A. M. Naylor-Olsen, W. M. Sanders, W. M. *Bioorg. Med. Chem. Lett.* **1997**, *7,* 67–72.
31. D. W. Banner, P. Hadvary, P. *J. Biol. Chem.* **1991**, *266,* 20085–20093.
32. S. Okamoto, A. Hijikata, R. Kikumoto, S. Tonomura, H. Hara, K. Ninomiya, A. Maruyama, M. Sugano, Y. Tamao, Y. *Biochem. Biophys. Res. Commun.* **1981**, *101,* 440–446.
33. J. Sturzebecher, F. Markwardt, B. Voigt, G. Wagner, P. Walsmann, *Thromb. Res.* **1983**, *29,* 635–642.
34. J. E. Ladbury, *Chem. Biol.* **1996**, *3,* 973–980.
35. P. R. Connelly, R. A. Aldape, F. J. Bruzzese, S. P. Chambers, M. J. Fitzgibbon, M. A. Fleming, S. Itoh, D. J. Livingston, M. A. Navia, J. A. Thomson, *Proc. Natl. Acad. Sci. U. S. A* **1994**, *91,* 1964–1968.
36. D. Ringe, *Curr. Opin. Struct. Biol.* **1995**, *5,* 825–829.
37. R. Krishnan, I. Mochalkin, R. Arni, A. Tulinsky, *Acta Cryst.* **2000**, *D56,* 294–303.
38. H. Brandstatter, D. Turk, H. W. Hoeffken, D. Grosse, J. Sturzebecher, P. D. Martin, B. F. Edwards, W. Bode, J. Mol. Biol. **1992**, *226,* 1085–1099.
39. G. Mlinsek, PhD Dissertation, **2004**, University of Ljubljana.

Povzetek

Trombin, serinska proteinaza iz družine tripsina, igra pomembno vlogo pri trombozi in hemostazi. Zaradi potrebe po učinkovitih, hitro delujočih, stabilnih in selektivnih direktnih trombinskih zaviralcih z možnostjo oralne uporabe, so raziskave na tem področju intenzivne. Pred kratkim smo z uporabo paradigme racionalnega načrtovanja odkrili dve seriji novih trombinskih zaviralcev. V prvi smo se osredotočili na aza peptidni skelet, ki posnema strukturo klasičnega tripeptida D Phe-Pro-Arg. V drugi pa smo iskali trombinske zaviralce z nevtralno P1 skupino, da bi s tem optimirali biološko razpoložljivost in selektivnost na tripsin. Kot rezultat naših prizadevanj smo dobili več bicikličnih mimetikov arginina na položaju P1, pripetih na glicil-prolinamidno in piridinon-acetamidno ogrodje. V članku poročamo o sedmih kristalnih strukturah iz serije kongenernih zaviralcev z novim aza peptidnim ogrodjem in z nevtralno P1 skupino v kompleksu s trombinom. V diskusiji smo se osredotočili predvsem na prepoznavo obeh razredov zaviralcev v žepu S1 proteinskega aktivnega mesta, in sicer z analizo elektronske gostote in strukture vode v žepu.